Available online at www.sciencedirect.com
SCIENCE DIRECT®
Journal of Magnetic Resonance 163 (2003) 64–72
JMR Journal of Magnetic Resonance
www.elsevier.com/locate/jmr

Efficient 5QMAS NMR of spin-5/2 nuclei: use of fast amplitude-modulated radio-frequency pulses and cogwheel phase cycling

Thomas Bräuniger,[a,*] Kevin J. Pike,[b] Robin K. Harris,[a] and P.K. Madhu[c]

[a] *Department of Chemistry, University of Durham, Durham DH1 3LE, UK*
[b] *Department of Physics, University of Warwick, Coventry CV4 7AL, UK*
[c] *Department of Chemistry, University of Southampton, Southampton SO17 1BJ, UK*

Received 22 November 2002; revised 16 March 2003

Abstract

We report here an efficient multiple-quantum magic-angle spinning (MQMAS) pulse sequence involving fast amplitude-modulated (FAM) radio-frequency pulses for excitation and conversion of five-quantum (5Q) coherences of spin-5/2 nuclei. The use of a FAM-I type pulse train for the conversion of 5Q into 1Q coherences proves to be easier to implement experimentally than the earlier suggested use of a FAM-II type sequence [J. Magn. Reson. 154 (2002) 280], while delivering at least equal signal enhancement. Results of numerical simulations and experimental ^{27}Al 5QMAS spectra of aluminium acetylacetonate for different excitation and conversion schemes are compared to substantiate these claims. We also demonstrate the feasibility of acquiring 5QMAS spectra of spin-5/2 systems using cogwheel phase cycling [J. Magn. Reson. 155 (2002) 300] to select the desired coherence pathways. A cogwheel phase cycle of only 57 steps is shown to be as effective as the minimum conventional nested 77-step phase cycle.

Keywords: Solid-state NMR; 5QMAS; FAM; Sensitivity enhancement; Cogwheel phase cycling; Aluminium-27

1. Introduction

The multiple-quantum magic-angle spinning (MQMAS) experiment, introduced by Frydman and Harwood [1] in 1995, allows the acquisition of high-resolution NMR spectra of quadrupolar nuclei with half-integer spin in solids, by refocusing the fourth-rank elements of the second-order quadrupolar Hamiltonian in spin space. The simplest MQMAS experiment [2,3] involves two radio-frequency (RF) pulses of constant amplitude and phase ("continuous-wave" pulses), and is commonly referred to as the *CW–CW* scheme. The first RF pulse excites all possible multiple-quantum (MQ) coherences, the desired coherence order being selected by appropriate phase cycling. The second RF pulse converts this MQ coherence into observable one-quantum (1Q) coherence after an evolution period t_1. The resulting two-dimensional (2D) MQMAS spectrum then correlates the conventional anisotropic MAS lineshape in the detection dimension with a high-resolution isotropic spectrum in the indirect dimension.

As the MQMAS technique is relatively straightforward to implement on standard MAS NMR hardware, it has found widespread applications in solid-state NMR of quadrupolar nuclei, mostly in the form of the three-quantum (3Q) experiment, which can be performed on all nuclei with half-integer spin $I \geqslant 3/2$. The 3Q as well as higher-order coherence experiments have successfully been employed in the characterisation of inorganic materials such as minerals, ceramics, catalysts, and glasses [4]. However, MQMAS NMR suffers from inherently low sensitivity, caused mainly by the inefficiency of the *CW* pulses in exciting higher-order coherences and later converting them to 1Q coherence. This is especially true for polycrystalline or amorphous samples, where the orientation-dependent quadrupolar

* Corresponding author. Present address: Universität Halle, Fachbereich Physik, 06199 Halle, Germany. Fax: +49-345-5527161.
E-mail address: braeuniger@physik.uni-halle.de (T. Bräuniger).

1090-7807/03/$ - see front matter © 2003 Elsevier Science (USA). All rights reserved.
doi:10.1016/S1090-7807(03)00124-1

frequencies are distributed over a wide range. The low sensitivity problem becomes progressively worse when attempting to observe higher coherence orders (five-, seven-, and nine-quantum) for nuclei with spin quantum numbers larger than 3/2. Nevertheless the acquisition of 5Q, 7Q, or 9Q spectra is of interest, as for most samples they may yield a substantial improvement in resolution [5]. For spin-5/2 systems, the best resolution has been achieved by so-called 5Q3Q spectra [6], where not the 1Q but the 3Q coherence is used for refocusing the second-order quadrupolar broadening. However, for experiments of this type, the lack of sensitivity is particularly severe.

Consequently, many efforts have been devoted to achieving better sensitivity for MQMAS spectroscopy. The majority of the strategies developed so far has been aimed at improving the efficiency of the MQ $\rightarrow$ 1Q conversion process. A number of pulse schemes replacing the simple *CW* conversion pulse has been suggested, the principles and applications of which have been discussed in recent review articles [7,8]. Signal enhancements of up to a factor of 3 have been reported by the use of conversion techniques relying on adiabatic passage mechanisms. These pulse schemes include rotationally induced adiabatic coherence transfer (RIACT) [9], double frequency sweeps (DFS) [10,11], and fast amplitude modulation (FAM) [12,13]. The FAM method approximates an amplitude modulation of appropriate frequency by a series of pulse pairs, with each of the pairs consisting of two pulses with a 180° phase shift between them. The simplest FAM pulse train (''FAM-I'') is formed by a block of pulse pairs of uniform duration, separated by constant interpulse delays. Such a FAM pulse train can induce a change in the coherence order of magnitude |2|, e.g., 3Q $\rightarrow$ 1Q. While the three techniques mentioned above were originally designed for spin-3/2 nuclei, it has been shown that DFS [14] and FAM [15,16] conversion also work for the acquisition of both 3Q and 5Q spectra of spin-5/2 nuclei, even though the spin physics for these nuclei is more complex because of the additional energy levels involved in the conversion process.

The utilisation of these enhancement techniques for improving excitation efficiency has been explored only very recently. It has been shown that for spin-3/2 nuclei, higher 3Q intensity can be obtained by preceding the RIACT [9] or RIACT–FAM sequence [17] by a FAM block lasting for a rotor period [18–20]. It was also demonstrated that population transfer induced by multiple frequency sweeps (MFS) can improve the initial generation of 3Q coherence for spins with $I = 5/2$ [21]. In a recent article, Goldbourt and Vega [22] have reported a novel excitation scheme for creating 5Q coherences of spin-5/2 nuclei, employing a *CW* pulse immediately followed by a train of simple FAM pulse pairs. The idea underlying this approach is to convert 3Q coherence generated by the initial *CW* pulse into the desired 5Q coherence by use of the FAM train, which induces a population transfer between the $|\pm 3/2\rangle$ and $|\pm 5/2\rangle$ energy levels. In the Goldbourt–Vega sequence, the subsequent 5Q $\rightarrow$ 1Q conversion is effected by means of amplitude-modulated RF pulses of the FAM-II type [15], consisting of a number of pulses of varying duration and alternating phase. Experimentally, this sequence was shown to give a 5Q signal enhancement of a factor of 2.3 over the simple 5QMAS experiment with two *CW* pulses [22].

To consecutively manipulate the populations across the outer and inner satellite transitions of a spin-5/2 nucleus (to give a total coherence order change of |4|), the FAM-II conversion pulse used by Goldbourt and Vega [22] is composed of two blocks of amplitude-modulated pulses with different pulse durations. Consequently, a large number of pulse program parameters needs to be optimised before the desired signal enhancement can be obtained, and this somewhat impairs the practical applicability of such a scheme. In this article, we demonstrate that the Goldbourt–Vega sequence can be simplified by using FAM pulse pairs with uniform pulse duration (FAM-I) for conversion. Numerical simulations suggest that the use of FAM-I pulse trains produces a 5Q signal enhancement at least equal, and in certain cases superior, to that of the Goldbourt–Vega sequence using FAM-II. The modified pulse sequence is also tested by acquiring 5Q spectra of the spin-5/2 nucleus ^{27}Al on a sample of aluminium acetylacetonate. The experimental results convincingly show that the use of a FAM-I type conversion pulse does not compromise the performance of the Goldbourt–Vega sequence, while considerably simplifying the practical implementation.

In addition, the application of cogwheel phase cycling to the acquisition of 5QMAS spectra is demonstrated. Cogwheel phase cycling, as recently proposed by Levitt et al. [23], allows the duration of phase cycles calculated according to conventional principles [24,25] to be greatly reduced, by incrementing the phase of irradiation blocks simultaneously. For example, the split-t_1 pulse sequence used for the 5QMAS experiments in this paper employs three pulse blocks and requires a minimum conventional phase cycle of 77 steps [23]. In contrast, the cogwheel phase cycling for the same experiment needs only 57 steps. The validity of the cogwheel approach for 5QMAS spectra is also shown experimentally by acquiring an ^{27}Al spectrum of aluminium acetylacetonate, using the 57-step phase cycle, and comparing it with one obtained using the minimum 77-step nested phase cycle.

2. FAM pulses in 5QMAS: classification and notation

Ideally speaking, the FAM train for the conversion of 5Q $\rightarrow$ 1Q coherence should be composed of two blocks

of pulses with different modulation frequencies [15], a faster one followed by a slower one, so that both the outer transitions and the inner transitions are manipulated. We may write the basic building block of a fast amplitude-modulated pulse train with uniform pulse durations (FAM-I) as $[\beta_x$–τ_w–$\beta_{\bar{x}}$–$\tau_w]$, where x and $\bar{x}$ are the phases of the pulses with a duration of β, separated by a delay of τ_w. The basic FAM pulse pair can be repeated several times, leading to a FAM block with a total number of pulses n. This block may be followed by another one with a different modulation frequency, i.e., with different values for β and τ_w. A block of FAM-II with 4 pulses, on the other hand, can be represented in the above notation as follows: $[\beta^1_x$–τ_w–$\beta^2_{\bar{x}}$–τ_w–β^3_x–τ_w–$\beta^4_{\bar{x}}]$. Here, β^1 equals the duration of the optimised *CW* conversion pulse in the *CW–CW* scheme and $\beta^1 > \beta^2 > \beta^3 > \beta^4$. A second FAM-II block, again with 4 pulses, of the form $[\beta^5_x$–τ_w–$\beta^6_{\bar{x}}$–τ_w–β^7_x–τ_w–$\beta^8_{\bar{x}}]$ may be added to the above block to mimic a different modulation frequency, where $\beta^5 > \beta^6 > \beta^7 > \beta^8$ and usually $\beta^1 > \beta^5 > \beta^2$. The number of pulses in each FAM block (and their duration) has to be optimised experimentally. In the 5Q experiment, both FAM-I and FAM-II may consist of two blocks of pulses with different modulation frequencies for the conversion pathway $5Q \rightarrow 3Q \rightarrow 1Q$ (as is the ideal case), or only one block with a single modulation frequency.

For a short yet precise notation of MQ pulse sequences involving fast amplitude-modulated pulses in either the excitation or conversion part, we denote a FAM train composed of several pulse blocks with differing modulation frequencies by $F^{\mathrm{I/II}}_{n,n'\ldots}$, where the Roman numeral in the superscript indicates FAM-I or FAM-II type of pulses. In the subscript, $n, n' \ldots$ correspond to the number of pulses in each FAM-I or FAM-II block. For example, $F^{\mathrm{I}}_{4,6}$ symbolises a FAM-I train with two blocks of different modulation frequencies, the first one having 4 pulses (two repetitions of the $x, \bar{x}$ pulse pair), and the second one having 6 pulses (three x, $\bar{x}$ pulse pairs). $F^{\mathrm{II}}_{4,6}$, on the other hand, symbolises a FAM-II train with two modulation blocks, the first one having 4 pulses, and the second one having 6 pulses of alternating phases and decreasing duration.

Following the convention to separate the excitation and conversion part by a hyphen, we can also incorporate the above notation into designations of full 5QMAS pulse sequences. The simple two-pulse experiment, as shown in Fig. 1a, is usually abbreviated to *CW–CW*, whereas a sequence using a FAM-I conversion pulse (Fig. 1b) may now be written as CW–F^{I}_n. The Goldbourt–Vega sequence [22] as drawn in Fig. 1c can be represented by CF^{I}_n–$F^{\mathrm{II}}_{4,4}$, where *CF* stands for a *CW* pulse followed by a FAM train. In the drawn example, the FAM-II conversion comprises two blocks of four pulses each, mimicking two different modulation frequencies. Our modification of the Goldbourt–Vega sequence is shown in Fig. 1d with a one-block FAM-I conversion and will be denoted by CF^{I}_n–$F^{\mathrm{I}}_{n'}$.

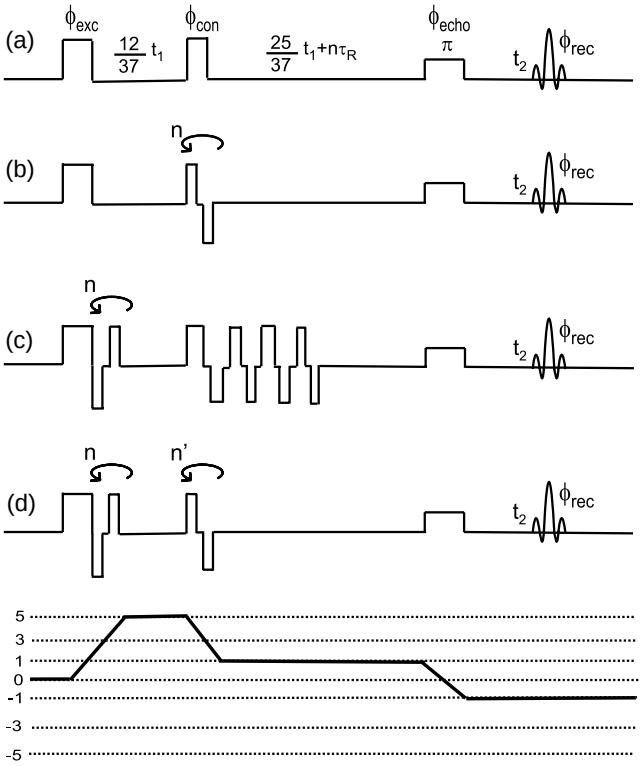

Fig. 1. Schematic representation of (a) the two-pulse MQMAS sequence (*CW–CW*), using continuous-wave RF pulses for both excitation and conversion of the MQ coherences; (b) the CW–F^{I}_n sequence; (c) the CF^{I}_n–$F^{\mathrm{II}}_{n',n''}$ sequence of Goldbourt and Vega [22]; (d) the CF^{I}_n–$F^{\mathrm{I}}_{n'}$ sequence suggested in this work, and below, the coherence pathway for the 5QMAS experiment. For details about the pulse sequence notation, see text.

3. FAM pulses in 5QMAS: computational results

The following pulse sequences were evaluated by numerical simulations with regard to the obtainable 5QMAS signal intensity: *CW–CW*, CW–F^{I}_n, CF^{I}_n–$F^{\mathrm{II}}_{n'}$, and CF^{I}_n–$F^{\mathrm{II}}_{n',n''}$ (two-block conversion), CF^{I}_n–$F^{\mathrm{I}}_{n'}$ and CF^{I}_n–$F^{\mathrm{I}}_{n',n''}$ (two-block conversion). A model spin-5/2 system with a nuclear quadrupolar coupling constant $\chi = (e^2qQ)/h = 6.0$ MHz and an asymmetry parameter $\eta = 0.5$ was used for these simulations. The respective 5Q echo intensities were calculated using the SIMPSON package [26] considering 232 powder orientations according to the ZCW scheme [27–29], and allowing a 5Q evolution time of 400 μs. As the efficiency of a MQ pulse sequence may depend markedly on the magnitude of the nuclear quadrupolar coupling constant, further simulations were performed for the above pulse schemes to evaluate the 5Q echo intensities as a function of χ. The detailed simulation parameters are given in Table 1, and the relevant SIMPSON input files are available from the corresponding authors upon request.

Table 1
Optimised parameters used for numerical simulations of the 5QMAS signal intensity

Spinning frequency	10 kHz
RF power	$\nu_1 = 100$ kHz
CW excitation pulse	4.5 μs
CW conversion pulse	2.1 μs
CF_n^{I} excitation pulse	$[4.5 + 4 \times (\overline{0.6}, 0.6)]$ μs
CF_n^{I} interpulse delay	0.2 μs
FAM-I conversion pulse, $F_{n'}^{\mathrm{I}}$	$5 \times (1, \overline{1})$ μs
FAM-I interpulse delay	1 μs
FAM-I conversion pulse, $F_{n',n''}^{\mathrm{I}}$	$[5 \times (0.4, \overline{0.4})]$ μs + $[5 \times (0.8, \overline{0.8})]$ μs
FAM-I interpulse delays, $F_{n',n''}^{\mathrm{I}}$	0.4 μs (first block), 0.8 μs (second block)
FAM-II conversion pulse, $F_{n'}^{\mathrm{II}}$	$2.1, \overline{1.4}, 0.8, \overline{0.5}$ μs
FAM-II conversion pulse, $F_{n',n''}^{\mathrm{II}}$	$[2.1, \overline{1.4}, 0.8, \overline{0.5}]$ μs + $[1.8, \overline{1.4}, 0.8, \overline{0.5}]$ μs
FAM-II interpulse delays	0.2 μs

Fig. 2a shows the 5Q echo obtained from the pulse sequences *CW–CW*, *CW*–F_n^{I}, CF_n^{I}–$F_{n'}^{\mathrm{I}}$, and CF_n^{I}–$F_{n'}^{\mathrm{II}}$, using only one-block FAM trains for coherence conversion. It is evident from the figure that the CF_n^{I}–$F_{n'}^{\mathrm{I}}$ type of sequence (here with $n = 8$ and $n' = 10$) is superior in performance to all the other pulse schemes. This is possibly due to the fact that the use of a single modulation frequency leads to a direct 5Q → 1Q coherence conversion. Since this process is adiabatic, the most efficient conversion pulse would be an adiabatic scheme, or in other words, a FAM-I type of scheme.

Fig. 2b shows the same plot with the pulse sequences using CF_n^{I} excitation now having FAM conversion pulse trains with two modulation blocks for an effective coherence transfer along the 5Q → 3Q → 1Q route. Such an approach enhances the 5Q echo further, but the best performance is still obtained for the CF_n^{I}–$F_{n',n''}^{\mathrm{I}}$ scheme. Notably, in this case, the CF_n^{I}–$F_{n',n''}^{\mathrm{II}}$ (Goldbourt–Vega) sequence performs almost as well. However, to reach this level of signal enhancement with the CF_n^{I}–$F_{n',n''}^{\mathrm{II}}$ scheme, optimal values for nine parameters need to be found.

Fig. 2c shows the echo response of the various sequences as a function of the nuclear quadrupolar coupling constant χ, with χ ranging from 3 to 10 MHz. With pulse sequence parameters optimised for $\chi = 6.0$ MHz, both CF_n^{I}–$F_{n'}^{\mathrm{I}}$ and CF_n^{I}–$F_{n'}^{\mathrm{II}}$ give substantially better results than the *CW*–F_n^{I} and *CW–CW* sequences for the χ range from 3 MHz to about 8 MHz, after which the performance becomes nearly equal unless further optimisations are done on the FAM trains.

Preliminary simulations of echo intensity at spinning speeds of 20 and 30 kHz (results not shown) indicate that the CF_n^{I}–$F_{n'}^{\mathrm{I}}$ sequence continues to give much higher intensity than the *CW–CW* scheme. The signal enhancement delivered by FAM-type sequences depends on the rotor speed via the induced level crossings in the energy diagram of the nucleus. However, the exact na-

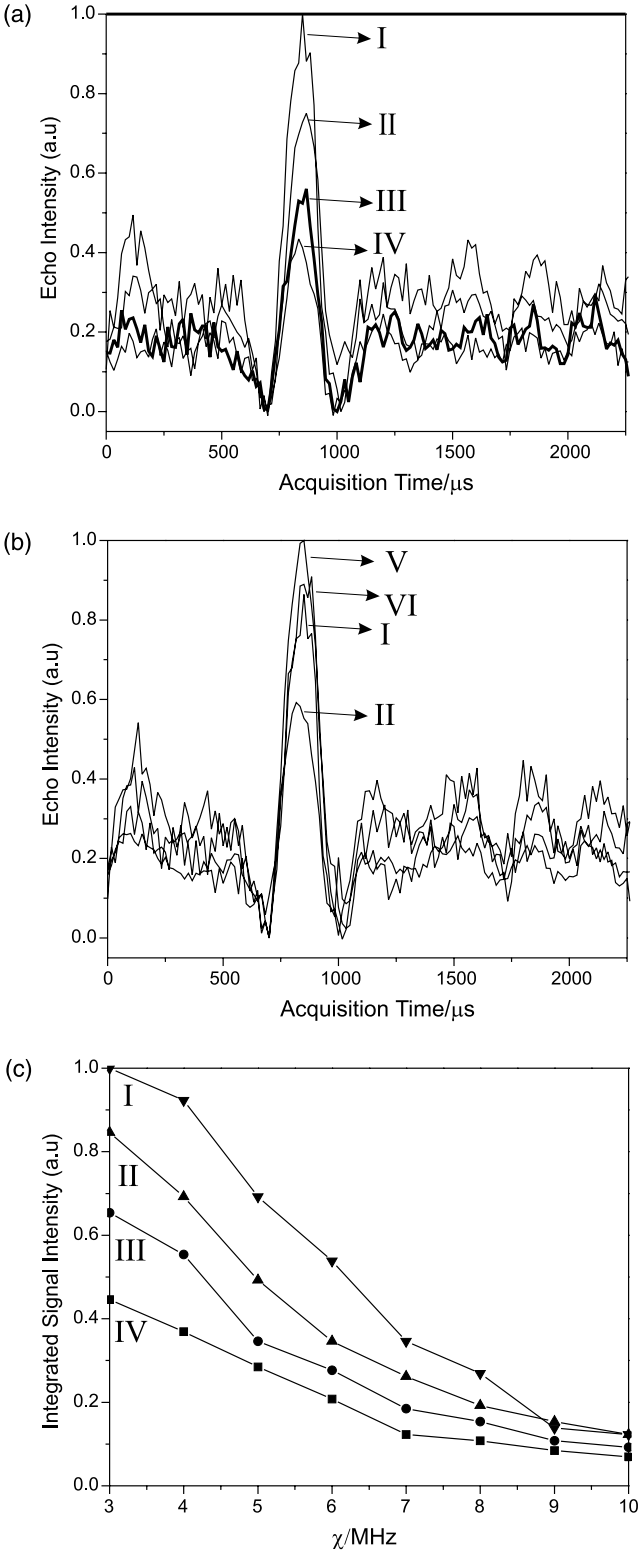

Fig. 2. Numerical simulation of the 5Q echo signal for the four pulse sequences shown in Figs. 1a–d. (a) Echo intensities for: (I) CF_n^{I}–$F_{n'}^{\mathrm{I}}$, (II) CF_n^{I}–$F_{n'}^{\mathrm{II}}$, (III) *CW*–F_n^{I}, and (IV) *CW–CW*. (b) Echo intensities for: (I) CF_n^{I}–$F_{n'}^{\mathrm{I}}$, (II) CF_n^{I}–$F_{n'}^{\mathrm{II}}$, (V) CF_n^{I}–$F_{n',n''}^{\mathrm{I}}$ (two-block conversion), (VI) CF_n^{I}–$F_{n',n''}^{\mathrm{II}}$ (two-block conversion), (c) Echo intensities as a function of the nuclear quadrupolar coupling constant χ, where the labels correspond to the legend given above for plot (a). The parameters used in the simulations are listed in Table 1.

ture and extent of this dependence will not be further explored in the context of this article.

The numerical simulations hence point to a superior efficiency of the CF_n^{I}–$F_{n'}^{\mathrm{I}}$ scheme, giving a performance comparable to the Goldbourt–Vega sequence with a two-block conversion pulse. Because of the reduced set of optimisable parameters, the experimental implementation of the CF_n^{I}–$F_{n'}^{\mathrm{I}}$ scheme is expected to be comparatively easy.

4. FAM pulses in 5QMAS: experimental results

To test the performance of the pulse sequences experimentally, we acquired ^{27}Al 5QMAS spectra of aluminium acetylacetonate, $Al(CH_3COCHCOCH_3)_3$, using the *CW*–*CW*, *CW*–F_n^{I}, and CF_n^{I}–$F_{n'}^{\mathrm{I}}$ sequences, respectively. All spectra were obtained on a Chemagnetics Infinity 600 spectrometer without proton decoupling, at a Larmor frequency of $\nu(^{27}\mathrm{Al}) = 156.37\,\mathrm{MHz}$, using a Chemagnetics MAS probe with a rotor diameter of 3.2 mm. The whole echo was acquired using the split-t_1 method [30,31], the idea of which is to prevent the migration of the echo in the acquisition time domain (t_2) by incorporating appropriate factors into the pulse program. The rate of the echo progression in t_2 is determined by the ratio k of second-order coefficients $C(I,m)$, which in turn depend on the spin quantum number I, and the coherence order m [1,7,8]. For spin $I = 5/2$ with $m = 5$, $k = 25/12$. Thus, as shown in Fig. 1a, the evolution time t_1 is split into two parts, namely $[1/(1+k)]t_1$ and $[k/(1+k)]t_1$, so that no shearing transformation is needed for the resulting spectrum. An additional delay of an integral number of rotor periods, $n\tau_{\mathrm{R}}$, was added to allow the acquisition of the whole echo, which ensures pure absorptive lineshapes in the 2D spectrum. A nested phase cycle with 160 steps (as listed in Table 2) was used to select the $\{0,+5,+1,-1\}$ coherence pathway. For the composite CF_n^{I} excitation scheme, the FAM train pulses need to be phase-cycled in conjunction with the *CW* pulse phase (i.e., $0° + \Phi_{\mathrm{exc}}$ and $180° + \Phi_{\mathrm{exc}}$), to prevent the mixing of unwanted coherences into the acquired signal.

Parameter optimisation was performed by running the 5QMAS pulse sequence in 1D mode (i.e., the first t_1 slice) with an interval of about 1 μs between excitation and conversion pulses, and then comparing the obtained echo intensities for different values of the parameter in question. For a FAM train, the pulse duration, the number of pulse pairs, and the interpulse delay constitute the optimisable parameters. In addition, the best value for the duration of the initial *CW* excitation pulse needs to be found. A sensible optimisation strategy is to obtain an appreciable 5Q signal first by finding the best RF pulse durations for the *CW*–*CW* sequence. Subsequently, the *CW*–F_n^{I} pulse program can be used to find the best values for the FAM conversion pulse, and finally the full CF_n^{I}–$F_{n'}^{\mathrm{I}}$ sequence with the additional modulation in the excitation part can be optimised. We found that re-optimising the excitation *CW* pulse after

Table 2
The 160 step nested phase cycle used for acquisition of the 5QMAS spectra shown in Fig. 3

Phase	Value/degrees
ϕ_{exc}	$(0,18,36,54,72,90,108,126,144,162,180,198,216,234,252,270,288,306,324,342)_8$
ϕ_{con}	$(0)_{160}$
ϕ_{echo}	$(0)_{20}$, $(45)_{20}$, $(90)_{20}$, $(135)_{20}$, $(180)_{20}$, $(225)_{20}$, $(270)_{20}$, $(315)_{20}$
ϕ_{rec}	$\{(0,270,180,90)_5,(90,0,270,180)_5,(180,90,0,270)_5,(270,180,90,0)_5\}_2$

Subscripts indicate the number of times the phase cycle in parentheses or brackets must be repeated.

Table 3
The experimental parameters used to acquire comparative ^{27}Al 5QMAS spectra of aluminium acetylacetonate for different pulse sequences (Fig. 3) and different phase cycling schemes (Fig. 5)

	Pulse sequences (Fig. 3)	Phase cycling (Fig. 5)
Data points ($t_2 \times t_1$)	1024×32	512×64
Dwell times ($\Delta t_2 \times \Delta t_1$)	$(10 \times 4)\,\mu\mathrm{s}$	$(10 \times 10)\,\mu\mathrm{s}$
RF power, ν_1	100 kHz	50 kHz
CW excitation pulse	4.5 μs	—
CW conversion pulse	2.0 μs	—
FAM-I conversion pulse	$1 \times (1.1, \overline{1.1})\,\mu\mathrm{s}$	$4 \times (1, \overline{1})\,\mu\mathrm{s}$
FAM-I interpulse delay	0.2 μs	1 μs
CF_n^{I} excitation pulse	$[4.0 + 2 \times (\overline{0.8}, 0.8)]\,\mu\mathrm{s}$	$[5.0 + 2 \times (\overline{0.8}, 0.8)]\,\mu\mathrm{s}$
CF_n^{I} interpulse delay	0.2 μs	0.5 μs
Echo pulse (RF power, ν_1)	7.5 μs (≈23 kHz)	10 μs (≈16 kHz)
Echo delay	$51 \times \tau_R = 5.1\,\mathrm{ms}$	$25 \times \tau_R = 2.5\,\mathrm{ms}$
Spinning frequency ($1/\tau_R$)	10 kHz	10 kHz
No. of transients in t_2	$160 \times 2 = 320$	nested: 231, cogwheel: 228
Relaxation delay	2.0 s	2.0 s
Reference compound	$AlCl_3$(aq) at 0 ppm	$AlCl_3$(aq) at 0 ppm

completing the full set-up may lead to a slight improvement in the signal intensity. The final, optimised values for all relevant pulse durations and delays are listed in Table 3. The acquired time domain data were processed following the methods outlined in [22,32].

The resulting ^{27}Al 5QMAS spectra of aluminium acetylacetonate are shown in Figs. 3b–d. Depicted are the 2D spectra with their anisotropic (f_2) and isotropic (f_1) projections on the left-hand side, and normalised f_2 slices of the 2D ridge on the right-hand side. When determining the integrated line intensities of these slices, we found that the CF_n^{I}–$F_{n'}^{\mathrm{I}}$ sequence (Fig. 1d) outperforms the *CW–CW* sequence (Fig. 1a) by a factor of 3, and the *CW*–F_n^{I} sequence (Fig. 1b) by a factor of 1.8. In addition, when comparing the anisotropic projections of the 5QMAS spectra to the single pulse MAS spectrum shown in Fig. 3a, it is clear that both *CW*–F_n^{I} and CF_n^{I}–$F_{n'}^{\mathrm{I}}$ deliver better lineshapes than *CW–CW*. The exact nature of the influence of modulated pulses on the lineshapes of spin-5/2 nuclei is not yet entirely understood. An extensive discussion of this issue for 3Q spectra of spin-3/2 nuclei can be found in [17]. For the present case, the better lineshapes observed for the modulated pulse sequences may qualitatively be ascribed to the ability of the FAM pulses to excite and convert MQ coherences for a more representative set of differently oriented crystallites in the powder.

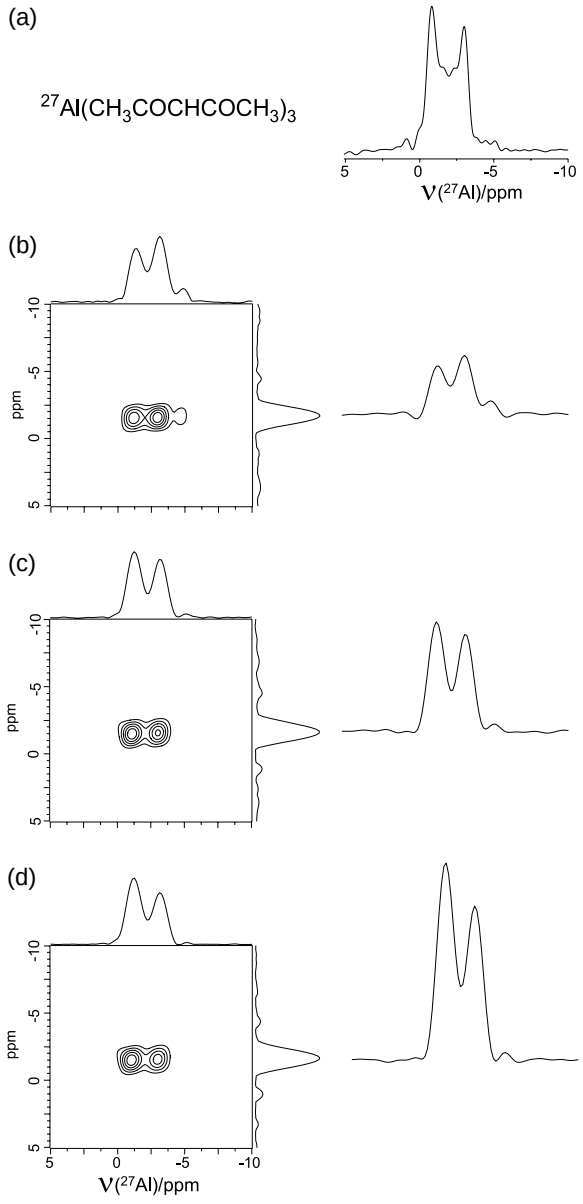

Fig. 3. ^{27}Al NMR spectra of aluminium acetylacetonate, Al(CH$_3$COCHCOCH$_3$)$_3$: (a) single-pulse MAS spectrum (32 transients, recycle delay 2 s, spinning frequency 10 kHz). The 5QMAS 2D spectra were acquired with the (b) *CW–CW*, (c) *CW*–F_n^{I}, and (d) CF_n^{I}–$F_{n'}^{\mathrm{I}}$ pulse sequences shown in Figs. 1a, b, and d, and with the experimental parameters listed in Table 3. The 2D contour plots and sky projections are shown on the left. The relevant anisotropic traces of the 2D ridge are plotted on the right in absolute intensity mode.

No direct experimental comparison of the new CF_n^{I}–$F_{n'}^{\mathrm{I}}$ sequence with the original CF_n^{I}–$F_{n'}^{\mathrm{II}}$ sequence of Goldbourt and Vega [22] was attempted, since the large number of experimental parameters of the FAM-II pulse train makes it very difficult to find an echo intensity maximum that can be considered global. However, the extensive numerical simulations described above can be taken as a strong indication of the fact that CF_n^{I}–$F_{n'}^{\mathrm{I}}$ is at least equal if not superior in performance to the original sequence, while being easier and faster to optimise. A possible explanation for the surprisingly good results obtained by this simplified pulse sequence can be sought in the nature of the direct 5Q → 1Q coherence conversion effected by a one-block FAM pulse. As mentioned above, this conversion process is adiabatic, and therefore, an adiabatic FAM-I train with uniform pulse durations seems to be working as efficiently as a two-block FAM-II train. Clearly, further work is needed to elucidate the details of adiabatic and non-adiabatic coherence transfer processes for spin-5/2 nuclei.

5. Cogwheel phase cycling for 5QMAS

A new concept of phase cycling, called cogwheel phase cycling, was introduced recently by Levitt et al. [23]. In conventional phase cycling, which is based on the work by Bain [24] and Bodenhausen et al. [25], the phases of the RF pulses or pulse trains are incremented consecutively, leading to a nested phase cycle. In contrast, the cogwheel approach involves simultaneous incrementation of the phases of the RF pulses, which leads to a marked reduction in the total number of phase cycling steps required for selection of a given coherence pathway.

The 160-step phase cycle listed in Table 2 is widely used for 5QMAS experiments. It allows the selection of

the coherence pathway $\{0,+5,+1,-1\}$ for all systems with spin $I \geqslant 5/2$, and involves phases that are easily and reliably realised on most spectrometers. However, the required minimum number of phase steps for a 5QMAS experiment is actually only 77, as can be shown in the following way. Defining the desired coherence transfer as Δp, an N-step phase cycle will select all coherence order changes $\Delta p \pm nN$, with $n = 0,1,2,\ldots$ [25]. In the case of 5QMAS, the desired change in the coherence order due to the excitation pulse is $\Delta p_{\mathrm{exc}} = +5$, with all other changes $\Delta p_{\mathrm{exc}} = -5,-4,\ldots,+4$ being undesired. A unique selection of $\Delta p_{\mathrm{exc}} = +5$ pathway can be obtained by an 11-step phase cycling of the excitation pulse, leading to a selection of coherence order changes given by $\Delta p = +5 \pm n \times 11$. This ensures that all the undesired pathways are suppressed. Similarly, if the phase of the conversion pulse ($\Delta p_{\mathrm{con}} = -4$) is kept constant at zero, the echo pulse ($\Delta p_{\mathrm{echo}} = -2$) needs to be phase cycled with at least seven steps, in order to exclude coherence order changes other than $\Delta p_{\mathrm{con}} + \Delta p_{\mathrm{echo}} = -6$. While the minimum number of nested phase cycle steps is hence $11 \times 7 = 77$, the minimum cogwheel cycle has only 57 steps.

For cogwheel phase cycles, the phase step with which each pulse and receiver is incremented can be written as $(2\pi/N)v$, where N is the number of phase cycle steps, and v is the *winding number* [23]. One of the solutions for the minimum 5QMAS cogwheel phase cycle of $N = 57$ steps can then be represented in a convenient notation by `COG57(-5,0,1;27)`. The first three numbers in brackets corresponds to the winding numbers of the three pulses in the 5QMAS pulse schemes, and the fourth number correspond to the winding number of the receiver. This concise representation, with phases defined by the winding numbers and the total number of steps, obliterates the need for writing explicit phase tables as is normally done.

For the case of the 5QMAS sequence under consideration, the number of phase steps N and the winding numbers may be obtained using the simple rules given by Levitt et al. [23]. The three independent RF segments of the sequence (excitation, conversion, and echo pulse) are denoted as A, B, and C. The order of coherences in the interval between A and B is represented by p^0_{AB}, similarly p^0_{BC} for the interval between B and C, and the maximum coherence order supported by the spin system is denoted as $p_{\max}$. We can then obtain the following relations [23]:

$$\begin{aligned} N &= (p_{\max}+1+|p^0_{AB}|)(p_{\max}+1+|p^0_{BC}|) - 4|p^0_{AB}p^0_{BC}|, \\ \Delta\nu_{AB} &= (signp^0_{AB})(p_{\max}+1-|p^0_{BC}|), \\ \Delta\nu_{BC} &= (signp^0_{BC})(p_{\max}+1-|p^0_{AB}|), \end{aligned} \tag{1}$$

where sign x is equal to 1 if $x \geqslant 0$ and is equal to -1 otherwise. In the above, $\Delta\nu_{AB} = \nu_B - \nu_A$ and $\Delta\nu_{BC} = \nu_C - \nu_B$. For the 5QMAS experiment in spin-5/2 systems, we have $p_{\max} = 5$, $p^0_{AB} = 5$, and $p^0_{BC} = 1$. This yields $N = 57$, $\Delta\nu_{AB} = 5$ and $\Delta\nu_{BC} = 1$. By fixing $\nu_B = 0$ (i.e., using a constant null phase for the conversion pulse), we then get $\nu_A = -5$ and $\nu_C = 1$. Following the master equation [25]

$$\sum_i \Delta p_i \phi_i + \phi_{\mathrm{rec}} = 0, \tag{2}$$

where Δp_i is the change in the coherence order induced by the ith pulse of phase ϕ_i, and ϕ_{rec} is the receiver phase, we get the winding number of the receiver in the case considered here as $\nu_{\mathrm{rec}} = 27$, since $\phi_{\mathrm{rec}} = (2\pi/N)\nu_{\mathrm{rec}}$.

Fig. 4 gives a diagrammatic illustration of the cogwheel phase cycle, `COG57(-5,0,1;27)`. This is a cogwheel selection diagram for the cycle with $\{N, \Delta\nu_{AB}, \Delta\nu_{BC}\} = \{57,+5,+1\}$. According to the cogwheel selection rules, feasible cogwheel cycles should satisfy the following inequality [23]:

$$(\Delta\nu_{AB}p_{AB} + \Delta\nu_{BC}p_{BC}) \neq (5\Delta\nu_{AB} + \Delta\nu_{BC}) + N \times \text{integer} \tag{3}$$

for all pathways $\mathbf{p} \neq \mathbf{p}^0$ which start at the coherence order 0, terminate at coherence order -1, and which pass through coherence orders such that $-5 \leqslant p_{AB} \leqslant +5$ and $-5 \leqslant p_{BC} \leqslant +5$. In the case being considered here, $\mathbf{p}^0 = \{0,+5,+1,-1\}$. The cogwheel selection diagram,

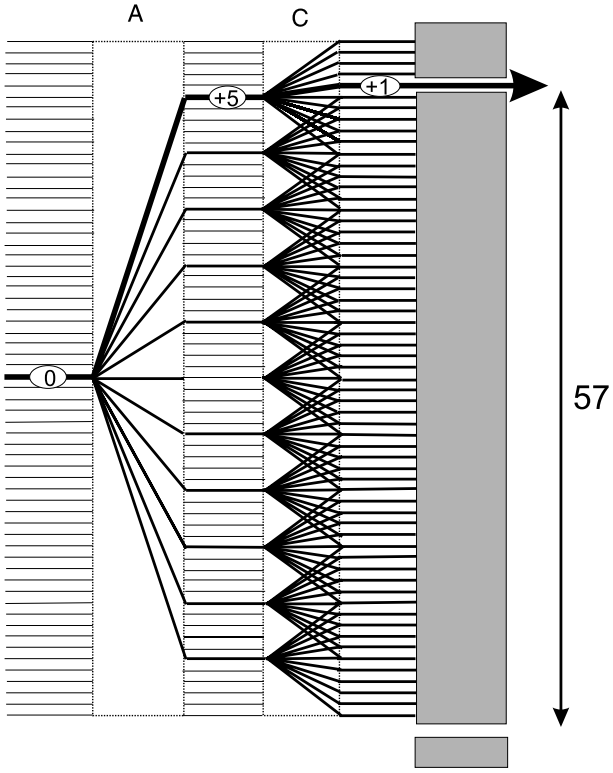

Fig. 4. Cogwheel selection diagram for the cogwheel phase cycle `COG57(-5,0,1;27)` used in the 5QMAS pulse sequence. The labels A and C indicate the respective RF blocks.

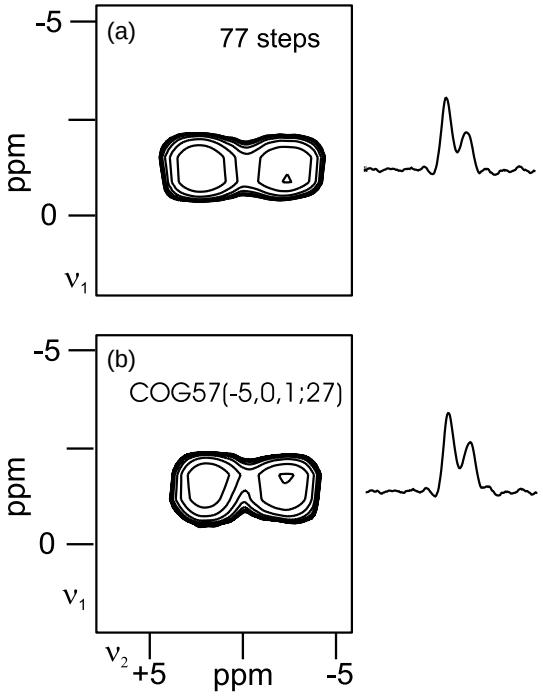

Fig. 5. ^{27}Al 5QMAS NMR spectra of aluminium acetylacetonate, $Al(CH_3COCHCOCH_3)_3$, acquired with the CF^I_n–$F^I_{n'}$ pulse sequence shown in Fig. 1d, using (a) the minimum nested phase cycle of 77 steps with 231 transients and (b) the cogwheel phase cycling scheme COG57(−5,0,1;27) with 228 scans. Also shown are the anisotropic traces of the 2D ridges.

Fig. 4, shows the possible values of $\Delta\nu_{AB}p_{AB} + \Delta\nu_{BC}p_{BC}$ plotted as horizontal levels. The construction of the levels is split into two steps, with level spacings in a 5:1 ratio that reflect the winding numbers $\Delta\nu_{AB} = +5$ and $\Delta\nu_{BC} = +1$. For the case shown here, the coherence orders p_{AB} and p_{BC} take all integer values between −5 and +5. Hence, each of the 10 branches splits into 10 subbranches. The barrier on the right has holes spaced by 57 units. This is just enough to clearly separate out the $\{p_{AB}, p_{BC}\} = \{+5, +1\}$ pathway from all the undesired ones.

Fig. 5 shows ^{27}Al 5QMAS spectra of aluminium acetylacetonate with both the minimum nested phase cycle steps and the cogwheel solution COG57(−5,0,1;27) acquired on the same Chemagnetics Infinity 600 spectrometer described above, but using a Chemagnetic MAS probe with a 4 mm rotor diameter. Both spectra were recorded with the new CF^I_n–$F^I_{n'}$ scheme, and the detailed experimental parameters are given in Table 3. The number of transients was $3 \times 77 = 231$ for the nested phase cycle and $4 \times 57 = 228$ for the cogwheel phase cycle. The anisotropic slices of the 5QMAS spectra clearly show that the selectivity is the same for both phase cycling schemes. The results also demonstrate the ability of modern spectrometers to generate the predominantly non-integer cogwheel phases with sufficient accuracy.

6. Conclusions

Two methods have been presented to make the acquisition of 5QMAS NMR spectra of spin-5/2 nuclei more efficient: (a) increasing the signal intensity by using a new pulse sequence employing amplitude-modulated RF pulses, and (b) shortening the required minimum phase cycle by adopting the new concept of cogwheel phase cycling.

We have shown that the 5QMAS pulse sequence for signal enhancement recently introduced by Goldbourt and Vega [22] can be conveniently simplified by using a FAM-I conversion scheme with uniform pulse durations instead of the rather complex FAM-II scheme used originally. The thus created CF^I_n–$F^I_{n'}$ sequence (Fig. 1d) retains the desired signal enhancement, and was demonstrated to be decisively more efficient than the *CW*–*CW* and *CW*–F^I_n pulse schemes by both experiment and simulation. While delivering equal or better 5Q echo intensity than the Goldbourt–Vega sequence, the CF^I_n–$F^I_{n'}$ scheme is easier to optimise and implement experimentally, by virtue of having a smaller number of adjustable parameters. Finding a good set of parameters for CF^I_n–$F^I_{n'}$ is therefore a fairly straightforward procedure, and the authors hope that this will facilitate the use of fast amplitude-modulated RF pulses in 5QMAS pulse sequences. The clear advantage of incorporating FAM trains into 5Q excitation and conversion pulses is the considerable increase in the signal intensity obtained. In addition, it has been reported before that the use of FAM conversion pulses in the acquisition of 3QMAS spectra leads to lineshapes that are less distorted than those obtained from *CW* conversion pulses [17,20]. In this work, the same effect was observed for 5QMAS lineshapes, underlining again the advantages of using FAM pulses for the acquisition of high-quality MQMAS spectra needed for the elucidation of quadrupolar parameters.

Furthermore, the application of cogwheel phase cycling [23] to the acquisition of 5QMAS spectra was successfully demonstrated on ^{27}Al spectra of aluminium acetylacetonate. By making the choice of the number of t_2 transients for large 2D spectra more flexible and thus reducing acquisition time, cogwheel phase cycling allows for a more effective set-up of 5QMAS experiments. Further work is in progress to extend the cogwheel approach to MQMAS of higher coherence orders for spins with $I > 5/2$, and to experiments of the MQNQ type [6], where drastic reductions of the phase cycle length are expected.

Acknowledgments

The authors are grateful to Amir Goldbourt, Shimon Vega, and Malcolm Levitt for helpful and interesting discussions, and to Andrew P. Howes for technical assistance with the spectrometer. T.B. and K.J.P. thank

the UK Engineering and Physical Sciences Research Council for fellowships under Grants GR/M 88341 and GR/N 29549, and PKM wishes to acknowledge the University of Southampton for support.

References

[1] L. Frydman, J.S. Harwood, Isotropic spectra of half-integer quadrupolar spins from bidimensional magic-angle spinning NMR, J. Am. Chem. Soc. 117 (1995) 5367–5368.
[2] A. Medek, J.S. Harwood, L. Frydman, Multiple-quantum magic-angle spinning NMR: a new method for the study of quadrupolar nuclei in solids, J. Am. Chem. Soc. 117 (1995) 12779–12787.
[3] G. Wu, D. Rovnyak, B. Sun, R.G. Griffin, High-resolution multiple quantum MAS NMR spectroscopy of half-integer quadrupolar nuclei, Chem. Phys. Lett. 249 (1995) 210–217.
[4] K.J.D. MacKenzie, M.E. Smith, Multinuclear Solid-State NMR of Inorganic Materials, Pergamon Press, Oxford, 2002.
[5] K.J. Pike, R.P. Malde, S.E. Ashbrook, J. McManus, S. Wimperis, Multiple-quantum MAS NMR of quadrupolar nuclei. Do five-, seven- and nine-quantum experiments yield higher resolution than the three-quantum experiment?, Solid State Nucl. Magn. Reson. 16 (2000) 203–215.
[6] A. Jerschow, J.W. Logan, A. Pines, High-resolution NMR of quadrupolar nuclei using mixed multiple-quantum coherences, J. Magn. Reson. 149 (2001) 268–270.
[7] L. Frydman, Fundamentals of multiple-quantum magic-angle spinning NMR on half-integer quadrupolar nuclei, in: D.M. Grant, R.K. Harris (Eds.), Encyclopedia of NMR, vol. 9, Wiley, Chichester, 2002.
[8] A. Goldbourt, P.K. Madhu, Multiple-quantum magic-angle spinning: high-resolution solid state NMR spectroscopy of half-integer quadrupolar nuclei, Chem. Month. 133 (2002) 1497–1534.
[9] G. Wu, D. Rovnyak, R.G. Griffin, Quantitative multiple-quantum magic-angle-spinning NMR spectroscopy of quadrupolar nuclei in solids, J. Am. Chem. Soc. 118 (1996) 9326–9332.
[10] A.P.M. Kentgens, R. Verhagen, Advantages of double frequency sweeps in static, MAS and MQMAS NMR of spin $I = 3/2$ nuclei, Chem. Phys. Lett. 300 (1999) 435–443.
[11] H. Schäfer, D. Iuga, R. Verhagen, A.P.M. Kentgens, Population and coherence transfer in half-integer quadrupolar spin systems induced by simultaneous rapid passages of the satellite transitions: a static and spinning single crystal nuclear magnetic resonance study, J. Chem. Phys. 114 (2001) 3073–3091.
[12] P.K. Madhu, A. Goldbourt, L. Frydman, S. Vega, Sensitivity enhancement of the MQMAS NMR experiment by fast amplitude modulation of the pulses, Chem. Phys. Lett. 307 (1999) 41–47.
[13] P.K. Madhu, A. Goldbourt, L. Frydman, S. Vega, Fast radio-frequency amplitude modulation in multiple-quantum magic-angle-spinning nuclear magnetic resonance: theory and experiments, J. Chem. Phys. 112 (2000) 2377–2391.
[14] D. Iuga, H. Schäfer, R. Verhagen, A.P.M. Kentgens, Population and coherence transfer induced by double frequency sweeps in half-integer quadrupolar spin systems, J. Magn. Reson. 147 (2000) 192–209.
[15] A. Goldbourt, P.K. Madhu, S. Vega, Enhanced conversion of triple to single-quantum coherence in the triple-quantum MAS NMR spectroscopy of spin-5/2 nuclei, Chem. Phys. Lett. 320 (2000) 448–456.
[16] T. Vosegaard, D. Massiot, P.J. Grandinetti, Sensitivity enhancement in MQ-MAS NMR of spin-5/2 nuclei using modulated rf mixing pulses, Chem. Phys. Lett. 326 (2000) 454–460.
[17] A. Goldbourt, P.K. Madhu, S. Kababya, S. Vega, The influence of the radiofrequency excitation and conversion pulses on the lineshapes and intensitites of the triple-quantum MAS NMR spectra of $I = 3/2$ nuclei, Solid State Nucl. Magn. Reson. 18 (2000) 1–16.
[18] H.-T. Kwak, S. Prasad, Z. Yao, P.J. Grandinetti, J.R. Sachleben, L. Emsley, Enhanced sensitivity in RIACT/MQ-MAS experiments using rotor assisted population transfer, J. Magn. Reson. 150 (2001) 71–80.
[19] K.H. Lim, T. Charpentier, A. Pines, Efficient triple-quantum excitation in modified RIACT MQMAS NMR for $I = 3/2$ nuclei, J. Magn. Reson. 154 (2002) 196–204.
[20] P.K. Madhu, M.H. Levitt, Signal enhancement in the triple-quantum magic-angle spinning NMR of spins-3/2 in solids: The FAM–RIACT–FAM sequence, J. Magn. Reson. 155 (2002) 150–155.
[21] D. Iuga, A.P.M. Kentgens, Triple-quantum excitation enhancement in MQMAS experiments on spin $I = 5/2$ systems, Chem. Phys. Lett. 343 (2001) 556–562.
[22] A. Goldbourt, S. Vega, Signal enhancement in 5QMAS spectra of spin-5/2 quadrupolar nuclei, J. Magn. Reson. 154 (2002) 280–286.
[23] M.H. Levitt, P.K. Madhu, C.E. Hughes, Cogwheel phase cycling, J. Magn. Reson. 155 (2002) 300–306.
[24] A.D. Bain, Coherence levels and coherence pathways in NMR. A simple way to design phase cycling procedures, J. Magn. Reson. 56 (1984) 418–427.
[25] G. Bodenhausen, H. Kogler, R.R. Ernst, Selection of coherence-transfer pathways in NMR pulse experiments, J. Magn. Reson. 58 (1984) 370–388.
[26] M. Bak, J.T. Rasmussen, N.C. Nielsen, SIMPSON: a general simulation program for solid-state NMR spectroscopy, J. Magn. Reson. 147 (2000) 296–330.
[27] S.K. Zaremba, Good lattice points, discrepancy, and numerical integration, Ann. Mater. Pure Appl. 4 (73) (1966) 293–317.
[28] H. Conroy, Molecular Schrödinger equation. VIII. A new method for the evaluation of multidimensional integrals, J. Chem. Phys. 47 (1967) 5307–5318.
[29] V.B. Cheng, H.H. Suzukawa Jr., M. Wolfsberg, Investigations of a nonrandom numerical method for multidimensional integration, J. Chem. Phys. 59 (1973) 3992–3999.
[30] S.P. Brown, S.J. Heyes, S. Wimperis, Two-dimensional MAS multiple-quantum NMR of quadrupolar nuclei. Removal of inhomogeneous second-order broadening, J. Magn. Reson. A 119 (1996) 280–284.
[31] S.P. Brown, S. Wimperis, Two-dimensional multiple-quantum MAS NMR of quadrupolar nuclei: a comparison of methods, J. Magn. Reson. 128 (1997) 42–61.
[32] Y. Millot, P.P. Man, Procedures for labeling the high-resolution axis of two-dimensional MQ-MAS NMR spectra of half-integer quadrupole spins, Solid State Nucl. Magn. Reson. 21 (2002) 21–43.